kov, Teor. i Experim. Khim. Akad. Nauk Ukr. SSR 4, 520 (1968).

[9]D. Grischkowsky and S. R. Hartmann, Phys. Rev. B 2, 60 (1970).

[10]Observations made during photon-echo experiments by N. A. Kurnit, I. D. Abella, and S. R. Hartmann [Phys. Rev. Letters 13, 567 (1964)] were subsequently interpreted in terms of an envelope-modulation effect by D. Grischkowsky and S. R. Hartmann [*ibid.* 20, 41 (1968)].

[11]In the subsequent argument the subscript k will be dropped whenever the inhomogeneous nature of the broadening is not explicitly involved.

[12]This is not the same as adopting the "interaction representation." The interaction representation sets up individual coordinate systems rotating with phase factors $e^{i\mathcal{H}_0 t/\hbar}$ for each of the eigenstates. Here we use common coordinate systems for the α states and for the β states, which rotate with phase factors $e^{i\omega t/2}$ and $e^{-i\omega t/2}$, respectively.

[13]A. L. Bloom, Phys. Rev. 98, 1105 (1955).

[14]The eigenfrequencies of $\hat{\mathcal{H}}_0$ will, of course, be given in the rotating coordinate system. For the α and β manifolds $\hat{\mathcal{H}}_0$ will thus consist of the relatively small diagonal elements $\hbar(\omega_{\alpha i}-\frac{1}{2}\omega)$, $\hbar(\omega_{\beta j}+\frac{1}{2}\omega)$.

[15]This time will generally be long compared with the phase memory time for a two-pulse echo. Modulation effects have been seen for ~100 μsec in the stimulated-echo envelope for a sample of lanthanum magnesium double nitrate doped with Ce^{3+} ions. The two-pulse phase memory in the same sample was ~ 3 μsec (unpublished observation).

[16]The tensor product $M_{1\alpha}\times M_{2\alpha}$ consists of two 2×2 submatrices $M_{1\alpha}$ and $M_{2\alpha}$ arranged on the diagonal of the 4×4 submatrix M. For a discussion of this formalism and for the theorem used later, see A. Messiah, *Quantum Mechanics* (Interscience, New York, 1961), p. 299.

[17]It is usually easier to detect small differences between the eigenfrequencies than to make a precise experimental measurement of the modulation amplitudes.

[18]It is difficult to generate microwave fields H_1 much in excess of 10 G in the low-Q cavities required for short-pulse experiments. Only those intervals which lie in a range $\sim 2\gamma H_1$ are effectively in resonance and are therefore able to contribute to the modulation effect.

PHYSICAL REVIEW B VOLUME 5, NUMBER 7 1 APRIL 1972

Paramagnetic Resonance of $^{155}Gd^{3+}$ in a ThO_2 Single Crystal: Study of the Hyperfine Structure (Allowed and Forbidden Lines)

G. Bacquet, J. Dugas, C. Escribe, L. Vassilieff
Laboratoire de Physique des Solides, Associé au Centre National de la Recherche Scientifique, 118, Route de Narbonne-31-Toulouse, France

and

B. M. Wanklyn
Clarendon Laboratory, Parks Road, Oxford, United Kingdom

(Received 12 October 1971)

The hyperfine structure of $^{155}Gd^{3+}$ ions in Th^{4+} substitutional cubic sites of a single crystal of ThO_2 (fluorite structure) has been studied by means of electron-paramagnetic-resonance techniques. The observation of "forbidden" transitions traditionally labeled by $\Delta m = 1$ or 2 is reported. Theoretical calculations using first-order perturbation theory for the hyperfine structure and nuclear Zeeman terms after a numerical diagonalization of the remaining (electronic Zeeman plus crystal-field terms) spin Hamiltonian are in good agreement with experimental results.

INTRODUCTION

The ground state of ions with half-filled shells (S-state ions) is an orbital singlet. When such ions are put in a crystal field, the spin degeneracy is partially removed. Although the electric field acting alone, regardless of its symmetry, cannot split in first order the S state, group-theory considerations[1] show that, even in a cubic field, the degeneracy will be split. Electron-paramagnetic-resonance (EPR) results concerning "cubic" spectra of Gd^{3+} ion ($4f^7$, $^8S_{7/2}$) substituted into tetravalent Th or Ce sites in thorium or cerium dioxydes[2-5] are in good agreement with Bethe's predictions. Forbidden fine-structure transitions with $|\Delta M| > 1$ were also observed. In the case of Gd^{3+}-doped CeO_2, Bir and Vinokurov[6] gave explicit expressions for the angular dependence of the positions and intensities of various forbidden fine-structure lines using first-order perturbation theory in $a/g\mu_B B$, where a is the constant representing the interaction with the crystal field. They only obtained a satisfactory agreement between theory and experiment for the line positions. Nevertheless, their theoretical formulas gave a correct over-all picture of the angular variation of intensity and of the position of intensity maxima and minima.

Previous experiments were done with naturalgadolinium-doped single crystals. Naturally occuring gadolinium contains two odd isotopes. These are ^{155}Gd and ^{157}Gd, each approximately 15% in abundance and each with nuclear spin $I=\frac{3}{2}$. Their respective hyperfine coupling constants have been determined in ThO_2 and CeO_2, but a detailed study of hyperfine structure (hfs) was impossible as all (even and odd) isotopes were present.

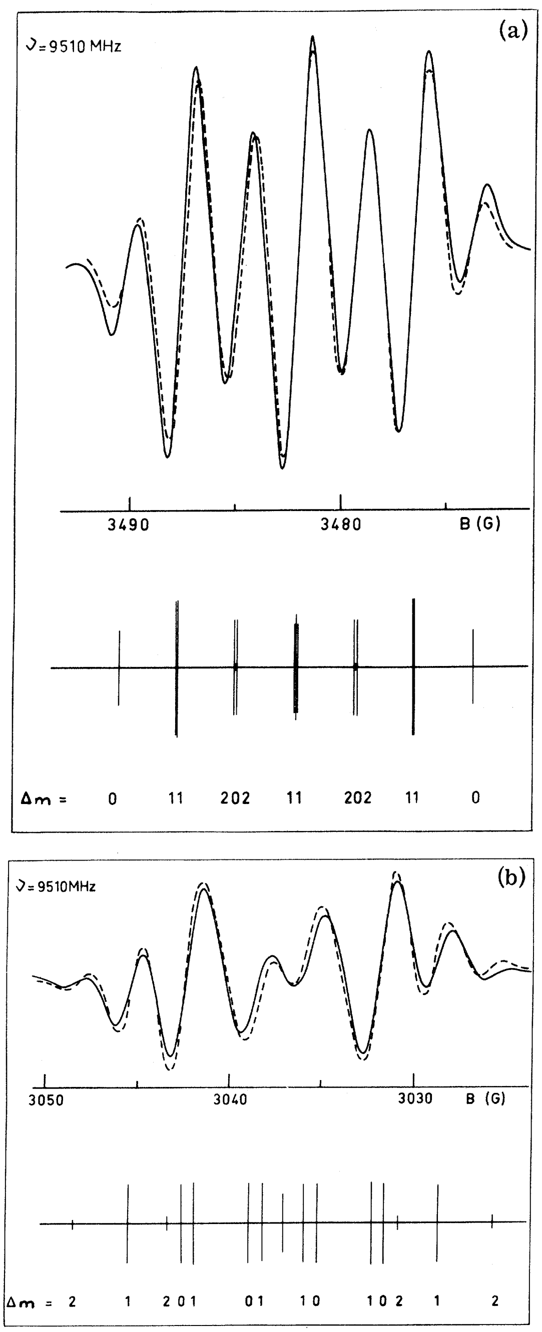

FIG. 1. Experimental (solid curve) and theoretical (dotted curve) spectra for (a) the ($M=-\frac{1}{2}\rightarrow\frac{1}{2}$) transition and (b) the ($M=\frac{1}{2}\rightarrow\frac{3}{2}$) transition, when the magnetic field is 20° away from the ⟨100⟩ direction in the (0$\bar{1}$1) plane. Lower parts indicate the relative intensities of various lines which contribute to theoretical spectra. The values 0, 1, or 2 of $|\Delta m|$ are indicated below the corresponding lines.

In this paper, we report EPR results concerning the hfs of $^{155}Gd^{3+}$ ions located in Th^{4+} cubic sites in thoria. So-called "forbidden" lines, the intensity of which is critically dependent on orientation of the crystal in the dc field, were observed in some fine-structure groups. They are due to a strong mixing between the eigenstates of the electron and nuclear Zeeman Hamiltonians. To deal with this problem, perturbation theory is generally used. Usually crystal-field plus hyperfine terms of the total spin Hamiltonian are considered to perturb the Zeeman levels. However, in our case, owing to the strength of the crystal field, such an approach cannot be used. A numerical diagonalization of the Zeeman plus crystal-field parts is needed. Only the hyperfine and nuclear Zeeman terms are taken as a perturbation. This procedure gives, in general, strongly mixed states and there are not rigorously forbidden transitions. We shall see in the following that the results of our calculations are in very good agreement with all the experimental data.

EXPERIMENTAL PROCEDURE AND RESULTS

The heavily doped (~0.1 wt% $^{155}Gd^{3+}$) ThO_2 single crystals used in this investigation were grown by one of us (B. M. W.) at the Clarendon Laboratory using the techniques described by Baker, Copland, and Wanklyn.[7] Room-temperature spectra were recorded using a conventional 100-kHz field-modulation X-band spectrometer built by two of us (G. B. and J. D.) at Toulouse. Two different spectra were observed: first, a trigonal one, the line positions of which critically depend on crystal orientation in the static field; determination of its "spin"-Hamiltonian parameters is impractical. Second, a cubic spectrum; in this case, the recordings obtained with the magnetic field parallel, respectively, to ⟨100⟩, ⟨111⟩, and ⟨011⟩ directions are similar to those previously quoted in the literature, except that each fine-structure transition is now split in four hyperfine lines, a weak line due to about 7% of residual even isotopes being always observed. Traces of ^{157}Gd may consequently be present, but they have undetectable effects on recorded spectra. A more interesting feature of spectra is the shape dependence of various groups of hyperfine lines upon orientation.[8] Extra lines can be seen especially in the ($M=-\frac{1}{2}\rightarrow\frac{1}{2}$), ($M=-\frac{3}{2}\rightarrow-\frac{1}{2}$), and ($M=\frac{1}{2}\rightarrow\frac{3}{2}$) fine-structure transitions. In the following, for the sake of simplicity, we shall speak of "allowed" and "forbidden" hyperfine lines, although these notations will show themselves quite improper.

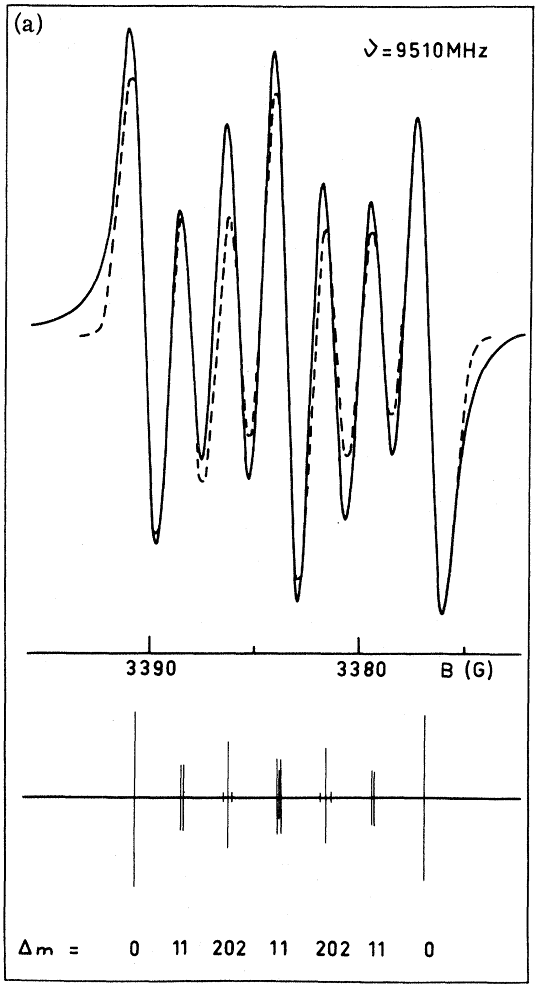

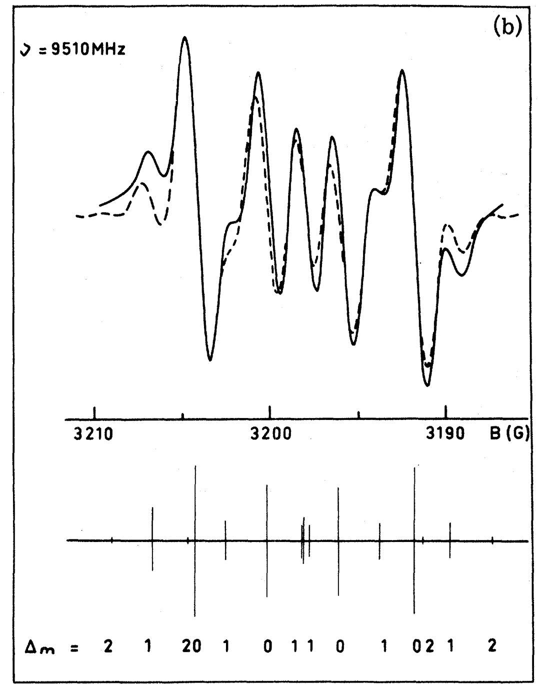

FIG. 2. Experimental (solid curve) and theoretical (dotted curve) spectra when $\theta = 70°$ in the $(0\bar{1}1)$ plane for (a) the $(M = -\frac{1}{2} \rightarrow \frac{1}{2})$ transition and (b) the $(M = -\frac{3}{2} \rightarrow -\frac{1}{2})$ transition. Lower parts indicate the relative intensities of various lines which contribute to theoretical spectra. The values 0, 1, or 2 of $|\Delta m|$ are indicated below the corresponding lines. Quadrupole coupling was taken into account.

In Figs. 1 and 2, parts of the total experimental spectra (full lines) corresponding to these three fine-structure transitions are shown for two different orientations: $\theta = 20°$ and $\theta = 70°$, where θ is the angle between the static field and the $\langle 100 \rangle$ direction in the $(0\bar{1}1)$ plane. The dotted curves are the theoretical ones, obtained as explained later. These two values of θ are chosen because they correspond to strong values of various "forbidden"-line intensities (cf. Figs. 3–5).

DISCUSSION

Abraham *et al.*[5] found that a spin Hamiltonian

$$\mathcal{H}_1 = g\mu_B \vec{B} \cdot \vec{S} + B_4(O_4^0 + 5O_4^4) + B_6(O_6^0 - 21O_6^4) \qquad (1)$$

cannot adequately describe their spectrum when the crystal was aligned with $\vec{B} \parallel \langle 100 \rangle$. The values $g, c \equiv 240B_4$ and $d \equiv 5040B_6$ obtained are quoted with errors larger than the experimental errors because they also reflect the inability of the Hamiltonian (1) to fit precisely the observed spectrum. This fact was confirmed by Copland's electron-nuclear double-resonance (ENDOR) studies of $^{157}Gd^{3+}$ in ThO_2 and CeO_2 single crystals.[9] His results were fitted to the usual spin Hamiltonian for S-state ions ($\mathcal{H}_{\text{Zeeman}} + \mathcal{H}_{\text{crystal field}} + \mathcal{H}_{\text{hfs}}$ including quadrupole term) to which have been added some other higher-order terms as suggested in principle by Koster and Statz[10] and generalized by Ray.[11]

As $^{155}Gd^{3+}$ ENDOR data are not available in the case of thoria, we were obliged to restrict our spin Hamiltonian to

$$\mathcal{H}_2 = g\mu_B \vec{B} \cdot \vec{S} + B_4(O_4^0 + 5O_4^4) + B_6(O_6^0 - 21O_6^4) + A\vec{I} \cdot \vec{S} - g_N \mu_N \vec{B} \cdot \vec{I}\,, \qquad (2)$$

where the used g_N value was that quoted in Varian NMR tables, and $S = \frac{7}{2}$, $I = \frac{3}{2}$. The best fit corresponds to the following values of the other parameters: $g = 1.9906 \pm 0.0005$, $c = -657.6 \pm 0.2$ MHz, $d = -4.15 \pm 0.1$ MHz, and $A = 12 \pm 0.05$ MHz.

When the external field is parallel to the $\langle 100 \rangle$ direction, which is the direction of Oz quantization axis, the energy eigenvalues can easily be determined. From the magnetic measurements, g, c, and d values were computed using the following relations:

$$B_{-5/2}-B_{7/2}=10c+3d-\frac{5}{8}c^2\left(\frac{1}{B_{7/2}}-\frac{1}{B_{-5/2}}\right)-\frac{85}{128}c^3\left(\frac{1}{B^2_{7/2}}-\frac{1}{B^2_{-5/2}}\right),$$

$$B_{-3/2}-B_{5/2}=-5c+7d+\frac{375}{256}c^3\left(\frac{1}{B^2_{-3/2}}-\frac{1}{B^2_{5/2}}\right), \tag{3}$$

$$B_{-1/2}-B_{3/2}=-6c+7d+\frac{5}{8}c^2\left(\frac{1}{B_{3/2}}-\frac{1}{B_{-1/2}}\right)-\frac{85}{128}c^3\left(\frac{1}{B^2_{-1/2}}-\frac{1}{B^2_{3/2}}\right),$$

$$B_0=B_{1/2}+\frac{35}{288}(3c-9d)^2\,\frac{1}{B_{1/2}},$$

and

$$g=h\nu/\mu_B B_0,$$

where c and d are expressed in G. The B_M are the values of magnetic field where the corresponding transitions appear. The $\mathcal{H}_1$ matrix was then diagonalized in the $|M\rangle$ basis, rotating the magnetic field (about the $\langle 0\bar{1}1\rangle$ axis) rather than the operator equivalents. To obtain numerical solutions for energy levels we used Jacobi's method applied to a sixteenth-order real matrix:

$$\mathcal{H}_1'=\begin{pmatrix}\mathrm{Re}(\mathcal{H}_1) & -\mathrm{Im}(\mathcal{H}_1)\\ \mathrm{Im}(\mathcal{H}_1) & \mathrm{Re}(\mathcal{H}_1)\end{pmatrix},$$

as explained by Durand.[12] This iterative method simultaneously gives the eigenvalues and the corresponding

$$|\Phi\rangle=\textstyle\sum_M C_M|M\rangle$$

eigenstates, but one must be careful because the convergence for the eigenvalues is faster than for the eigenstates. The theoretical angular dependence of each fine-structure transition only satisfactorily fits the experimental variations when the rate of change of these last is weak. Elsewhere, the discrepancy is always lower than 4%. The hyperfine structure was then studied using the Hamiltonian (2), where $A\vec{I}\cdot\vec{S}$ and the nuclear Zeeman term were taken as a perturbation. The eigenstates $|\Phi\rangle$ of $\mathcal{H}_1$ have a fourfold degeneracy with respect to m. To describe the zero-order eigenstates of $\mathcal{H}_2$ we used a basis $|\Phi,m\rangle$. For each $|\Phi\rangle$ numerical diagonalization of the obtained fourth-order matrix gives the four hyperfine energy levels and then the zero-order eigenstates of $\mathcal{H}_2$, which are expressed as

$$|\Psi\rangle=\sum_m C_m|\Phi\rangle|m\rangle=\sum_{m,M}a_{M,m}|M,m\rangle. \tag{4}$$

It must be emphasized that:

(i) The matrix element of the electron ladder operator $S_+=S_x+iS_y$ between two such states is given by

$$\langle\Psi_f|S_+|\Psi_i\rangle=\sum_{M,M',m,m'}a^*_{M',m'}a_{M,m}\delta_{M',m+1}\delta_{m',m}=\sum_{M,m}a^*_{M+1,m}a_{M,m},$$

which is, in general, different from zero, so that *all* the EPR transitions $i\to f$ are *a priori* allowed. Nevertheless, only the terms corresponding to $m'-m=0$ give a nonvanishing contribution.

(ii) The $a_{M,m}$ are functions of the dc field B in such a way that, in the limit $B\to\infty$, every $|\Psi\rangle$ becomes one of the $|M,m\rangle$ "pure"-spin states. It is now possible, for any value of B, to label such a $|\Psi\rangle$ by the notation $|\bar{M},\bar{m}\rangle$. Then one can write $\langle\Psi_f|S_+|\Psi_i\rangle=\langle\bar{M}_f,\bar{m}_f|S_+|\bar{M}_i,\bar{m}_i\rangle$, which is generally different from zero, even when $\Delta m\equiv m_f-m_i=0$. The transitions corresponding to $|\Delta M|\equiv|M_f-M_i|=1$ and $|\Delta m|=0$ are traditionally called "allowed"; those for which $|\Delta m|\neq 0$ are called "forbidden."

From such $|\Psi\rangle$ we computed the angular dependence of various transition probabilities and corresponding hyperfine-line positions. These results show that, in the four $(M=\pm\frac{7}{2}\leftrightarrows\pm\frac{5}{2})$, $(M=\pm\frac{5}{2}\leftrightarrows\pm\frac{3}{2})$ transitions, the various "forbidden" hyperfine lines are weak enough to be experimentally undetectable. Figures 3–5 show the theoretical curves we obtained in the case of the three other fine-structure transitions, where they are well observed.

An interesting feature of these results is that the various intensities critically depend upon orientation: It can be seen, in the $(M=-\frac{1}{2}\to\frac{1}{2})$ transition [Fig. 4(b)] that, around $\theta=25°$, $|\Delta m|=1$ and also $|\Delta m|=2$ "forbidden" lines have intensities greater than the $|\Delta m|=0$ "allowed" ones. The computed intensities of $|\Delta m|=3$ "forbidden" lines are very weak, $\lesssim 0.5\%$ of the most intense line. They have not been reported in the figures, and have no effect on recorded spectra. In each fine-structure transition, the hyperfine-line positions are given with respect to the line due to gadolinium

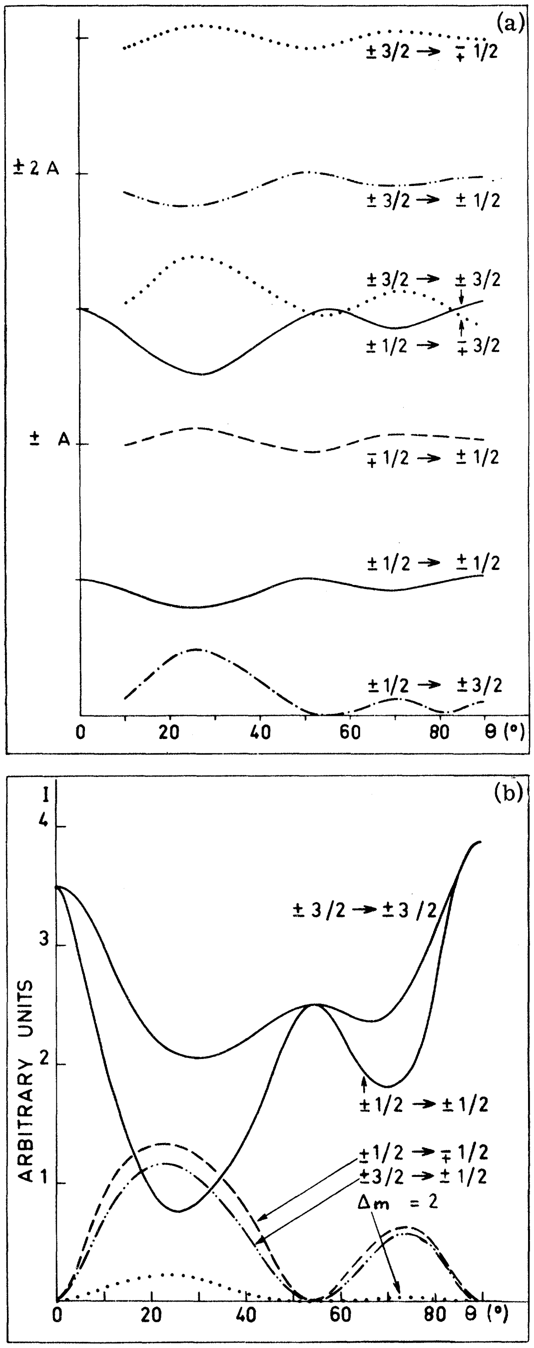

FIG. 3. Theoretical angular dependence of (a) hyperfine-line positions and (b) line intensities for the ($M=-\frac{3}{2}\rightarrow-\frac{1}{2}$) transition.

without nuclear spin.

As comparison between theory and experiment for each line was impossible owing to the strong overlapping of neighboring lines (the individual linewidth is equal to 1.3 G), the theoretical spectra were machine drawn using addition of derivatives of Gaussian lines. Computed intensity values were multiplied by a scale factor to obtain exact superposition with a line taken as a reference. The presence of a small amount (~ 7%) of gadolinium without nuclear spin was taken into account.

Figures 1 and 2 compare experimental and theoretical spectra for $\theta = 20°$ and $\theta = 70°$ where the intensities of "forbidden" lines are such that observed spectra are quite different from those usually expected. The lower parts of these figures explain how the theoretical spectra are built. It can be seen that both experimental and theoretically predicted shapes are the same. Nevertheless, there are some slight discrepancies concerning some lines positions and intensities. These results hold through the complete angular variation

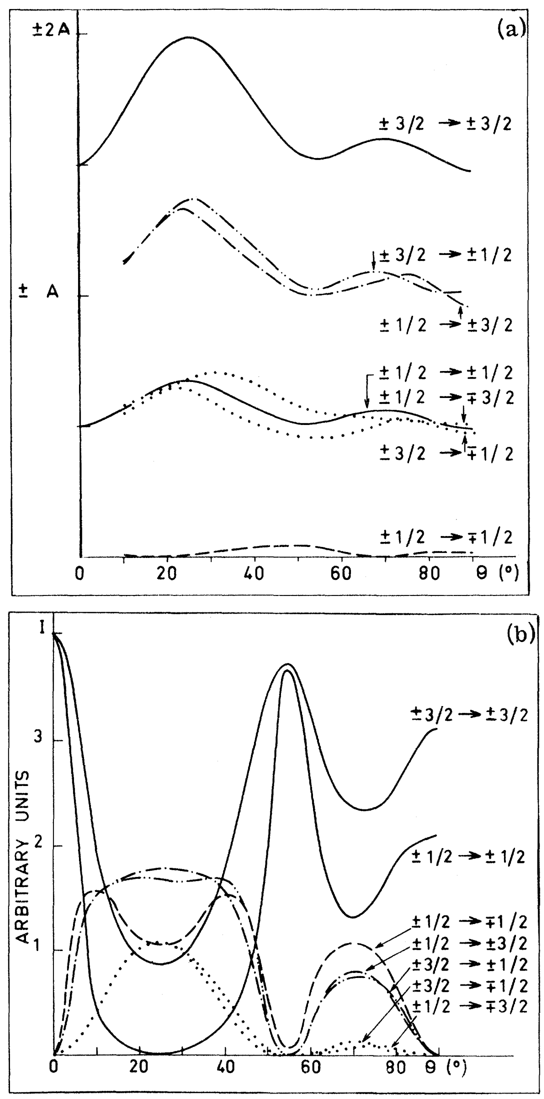

FIG. 4. Theoretical angular dependence of (a) hyperfine-line positions and (b) line intensities for the ($M=-\frac{1}{2}\rightarrow\frac{1}{2}$) transition.

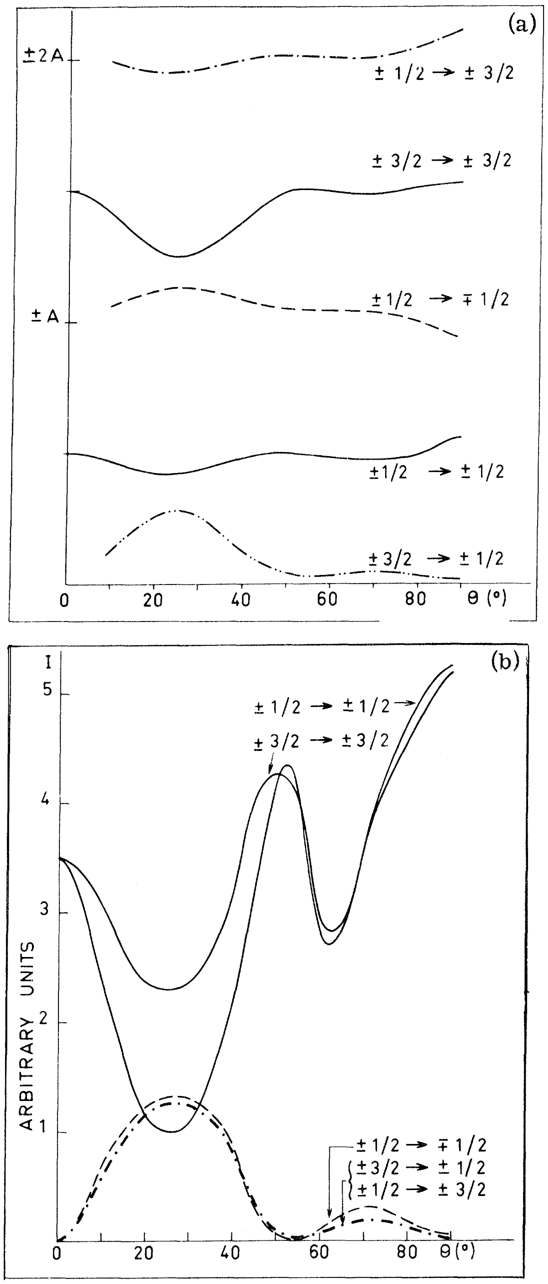

FIG. 5. Theoretical dependence of (a) hyperfine-line positions and (b) line intensities for the $(M=\frac{1}{2}\rightarrow\frac{3}{2})$ transition.

for each of the seven groups of hyperfine lines.

We were unsuccessful in determining the quadrupole-coupling-constant value. Including a quadrupole term in the spin Hamiltonian has only an unappreciable effect, as checked (cf. Fig. 2) using a quadrupole constant value ~ − 2 MHz extrapolated from Copland's results.[9] The major part of the discrepancy arises from possible crystal misalignment inside the cavity.

The existence of "forbidden" hyperfine lines has been known since Bleaney and Ingram[13] observed those occurring in the paramagnetic spectra of Mn^{2+} in several crystals of axial symmetry. The quadrupole interactions for several rare-earth ions were found by measuring the $|\Delta m| = 1, 2$ transitions in some of the early work on ethyl sulfates, as quoted by Bowers and Owen.[14]

In the aim to theoretically explain their existence, most of the authors who dealt with this problem used perturbation theory. In the case of axial symmetry Bleaney and Ingram found that "forbidden" lines are due to the mixing of hyperfine states by the interaction of the axial-field splitting D with the hyperfine interaction. However, Bleaney and Rubins[15] pointed out that this mixing should occur whenever the magnetic field is not directed along an axis of twofold or higher symmetry. Later on Drumheller and Rubins[16] observed the "forbidden" $|\Delta m| = 1$ lines of Mn^{2+} in the cubic field of MgO, and showed that they are due to hyperfine mixing with the zero-field cubic splitting a. They considered second-order admixture, and found that the approximated eigenstates are given by

$$|\Psi(M,m)\rangle = |M,m\rangle + \alpha(M)|M,m+1\rangle + \beta(M)|M,m-1\rangle \ . \quad (5)$$

From these states they calculated the intensity of "forbidden" $|\Delta m| = 1$ lines that show a $(\sin 4\theta)^2$ dependence. They also evaluated the splittings of the "forbidden" doublets to third-order perturbation theory, and both the intensities and the splittings agreed very well with their experimental data.

If, in the case of Mn^{2+}, splittings due to hyperfine structure are greater than those occurring from the fine structure, the situation is reversed for $^{155}Gd^{3+}$ in ThO_2, where the cubic crystal field cannot be considered as a perturbation of the Zeeman term, although the trigonometric functions which can be obtained by such an approach give adequate qualitative results for the outer $|\Delta m| = 1$ lines in the $(M=-\frac{1}{2}\rightarrow\frac{1}{2})$ transition.[17]

The obtained hyperfine coupling constant is very weak (12 MHz) and, for a given quadruplet, the hyperfine levels are so close that each of them is generally an admixture of the four $|m\rangle$. Our results agree with the conclusion of Drumheller and Rubins, i.e., "forbidden" lines arise from hyperfine mixing with the zero-field cubic splitting. However, the second-order admixture they proposed, is not sufficient to explain the appearance of $|\Delta m| = 2$ "forbidden" lines, as well as the observed angular dependence of intensities.

To deal with these last two points, a slightly different theoretical treatment was given by Bir, Butikov, and Sochava,[18] who tested it using Eu^{2+}-doped CaF_2 single crystals. But owing to the complexity of their experimental spectra, this test was only limited to 2×3 hyperfine lines (allowed and forbidden) in the $(M=-\frac{1}{2}\rightarrow\frac{1}{2})$ fine-structure transition for $^{151}Eu^{2+}$.

To conclude, we can say that the good agreement between the experimental and computed spectra we obtained shows the validity of the method we used, and it is not certain that a full diagonalization of the 32×32 matrix of the total spin Hamiltonian would considerably improve the results.

ACKNOWLEDGMENTS

The authors are indebted to Dr. J. M. Baker of the Clarendon Laboratory of Oxford for reading the manuscript and for his suggestions. We also acknowledge helpful discussions with Professor P. Gautier during the course of this work. The preparation of the single crystals of thoria was supported by the Science Research Council of the United Kingdom.

[1]H. A. Bethe, Ann. Physik 3, 133 (1929).
[2]W. Low and D. Shaltiel, J. Phys. Chem. Solids 6, 315 (1958).
[3]M. M. Abraham, E. J. Lee, and R. A. Weeks, J. Phys. Chem. Solids 26, 1249 (1965).
[4]I. V. Vinokurov, Z. N. Zonn, and V. A. Ioffe, Fiz. Tverd. Tela 7, 1012 (1965) [Sov. Phys. Solid State 7, 814 (1965)].
[5]M. M. Abraham, L. A. Boatner, C. B. Finch, E. J. Lee, and R. A. Weeks, J. Phys. Chem. Solids 28, 81 (1967).
[6]G. L. Bir and I. V. Vinokurov, Fiz. Tverd. Tela 7, 3392 (1965) [Sov. Phys. Solid State 7, 2730 (1966)].
[7]J. M. Baker, G. M. Copland, and B. M. Wanklyn, J. Phys. C 2, 862 (1969).
[8]G. Bacquet, J. Dugas, M. Bonnet, and C. Escribe, Compt. Rend. 270, 1961 (1970).
[9]G. M. Copland, thesis (University of Oxford, 1967) (unpublished).
[10]G. F. Koster and H. Statz, Phys. Rev. 113, 445 (1959); 115, 1568 (1959).
[11]T. Ray, Proc. Roy. Soc. (London) A227, 269 (1964).
[12]E. Durand, in *Solutions Numériques des Equations Algébriques*, (Masson, Paris, 1961). Vol. 2.
[13]B. Bleaney and D. J. E. Ingram, Proc. Roy. Soc. (London) A205, 336 (1951).
[14]K. D. Bowers and J. Owen, Rept. Progr. Phys. 18, 304 (1955).
[15]B. Bleaney and R. S. Rubins, Proc. Roy. Soc. (London) 77, 103 (1961).
[16]J. E. Drumheller and R. S. Rubins, Phys. Rev., 133, A1099 (1964).
[17]G. Bacquet, M. Bonnet, J. Dugas, and C. Escribe, in *Proceedings of the Sixteenth Colloque Ampère, Bucharest*, 1970, edited by I. Ursu (Academy of the Socialist Republic of Romania, Bucharest, Romania, 1971).
[18]G. L. Bir, E. I. Butikov, and L. S. Sochava, Fiz. Tverd. Tela 6, 2478 (1964) [Sov. Phys. Solid State 6, 1966 (1965)].

PHYSICAL REVIEW B VOLUME 5, NUMBER 7 1 APRIL 1972

Wave Theory of Lattice-Directed Trajectories. III. The Classical Limit

Hans C. H. Nip* and J. C. Kelly
Materials Irradiation Group, School of Physics, The University of New South Wales, Sydney 2033, *Australia*
(Received 1 September 1971)

We consider the applicability of classical mechanics to lattice-directed trajectories and obtain a projectile-energy-independent condition. A critical angle for channeling is obtained without the introduction of a continuum-wall approximation to the interaction potential. We derive an interaction equation in terms of relativistic particle mechanics from the conservation of energy and angular momentum. We also show by separation of variables in a former equation the containment of this classical theory by the previously developed wave treatment of lattice-directed trajectories.

I. INTRODUCTION

During the last decade a basically simple and effective classical theory has been developed[1] from the framework suggested by Lindhard[2] and Erginsoy[3] to explain the pronounced directional penetration anisotropy of energetic projectiles in thin single crystals. Various attempts have been made to develop a comprehensive wave-mechanical treatment similar to the wave theory of particle diffraction,[4] but the transition of these complex many-beam models to the classical model is not readily made. In two earlier papers[5,6] we developed and applied a relativistic quantum theory which is easily seen to contain the diffraction treatment[4] and the classical model.[1-3] In this paper we will examine the applicability of classical mechanics, the resulting classical model, and the correspon-